REPORT NO. 116
APRIL, 1958.

THE COLLEGE OF AERONAUTICS

CRANFIELD

The Exact Flow Behind a Yawed Conical Shock ¤

- by -

Flight Lieutenant G. Radhakrishnan, I.A.F.,
B.Sc.(Eng)., D.C.Ae., A.M.I.E.(Ind).

SUMMARY

The exact flow behind a yawed conical shock wave is investigated. A simple numerical method of solving the differential equations of motion behind the shock wave is evolved.

This method is applied to the case of the flow of a perfect gas behind a conical shock of semi-apex angle 30° yawed at 20° to a free stream of Mach number 10. The shape of the body which would produce such a shock wave is determined. The properties of the flow between the shock wave and the body surface are investigated particularly with respect to the variation of entropy and the streamline pattern.

The existence of a singular generator on the body surface in the plane of yaw and on the "leeward" side, at which the entropy is many-valued is brought out. It is found that, downstream of the shock, all stream lines curve round and tend to converge to this singular generator.

The body obtained by the present investigation is compared to the yawed circular cone which according to Stone's first order theory would produce the same shock wave dealt with in this particular case.

¤ Based on a thesis submitted in partial fulfilment of the requirements for the Diploma of The College of Aeronautics.

LIST OF CONTENTS

LIST OF SYMBOLS

a	Speed of sound.
C_p	Specific heat at constant pressure.
C_v	Specific heat at constant volume.
C_P	Pressure coefficient $= \frac{2}{\gamma M^2} (p/p_1 - 1)$.
h	Enthalpy $= C_p T$.
h	Interval between successive values of the independent variable x. . $h = x_{n+1} - x_n$ (in Appendix A)
p	Pressure.
q	Flow velocity.
$q_{max.}$	Absolute velocity (of gas discharging into vacuum)
M	Mach Number.
r	radial co-ordinate in Spherical polar system.
R	gas constant $= C_p - C_v$.
S	Entropy.
T	Absolute temperature.
V_1	Freestream velocity.
x	independent variable.
y	dependent variable.
(r, ψ, ω)	Spherical polar co-ordinates.
(u, v, w)	Components of velocity.
u	Component positive in direction r increasing.
v	Component positive in direction ψ increasing.
w	Component positive in direction ω increasing.

List of Symbols contd.

α	Angle of yaw or incidence.
γ	Ratio of specific heats $= \frac{C_p}{C_v}$.
ϵ	Equivalent shock wave angle.
ρ	Density.
ψ_w	Shock cone semi-apex angle.

SUBSCRIPTS.

w	Pertaining to shock wave.
s	Pertaining to solid body surface.
o	Pertaining total or stagnation conditions.
1	Pertaining to freestream (and upstream side of shock wave).
2	Pertaining to downstream side of shock wave.
3,4,5,etc.	Pertaining to successive ψ-wise steps chosen for numerical process of solution of differential equations.

1. INTRODUCTION.

The problem of supersonic flow around a yawed circular cone has received considerable attention in recent times but is still only partially solved. A comprehensive survey of the existing state of knowledge in this field was given in 1956 by Woods (Refence 1.). Several methods of solution have been proposed, but the first and second order theories developed by Stone seem to have had the widest application.

In a paper published in 1948 Stone (Ref.2) dealt with the problem by treating the flow as the sum of the non-yaw flow, exactly solved by Taylor and Maccoll in 1933 (Ref. 3) and a small perturbation due to yaw (included in the solutions as first order terms in α, the angle of yaw). In a later paper, published in 1951 (Ref. 4) he developed a second order theory. Extensive tables based on Stone's theory have been prepared at M.I.T. by Kopal and published as companion volumes to the tables of axi-symmetric flow around cones. (Refs. 5, 6, 7). These tables cover a wide range of Mach number and cone apex angle.

Stone's work has met with a certain amount of criticism mainly on two counts. One objection was on the grounds that the system of co-ordinates (using wind axes) used originally by Stone and subsequently by Kopal in the preparation of the M.I.T. tables was inconvenient to employ in practice. A detailed discussion of this aspect of the problem was given by Roberts and Riley (Ref. 8) who also laid down a procedure to modify the Stone solutions (as tabulated by Kopal) to more practical co-ordinates (using body axes).

The other was an important theoretical objection. Stone's first order theory implies a periodic variation of entropy around the circumference of the yawed cone. Thus the entropy varies from a maximum value at the "windward" generator to a minimum value on the "leeward" generator. Ferri pointed out in 1950 (Ref.9) that this contradicts the requirement that the solid cone surface must be a stream surface and therefore itself a surface of constant entropy. He discussed the flow around the cone in the general case and showed the existence of singular points along the "leeward" generator on which the entropy is many valued and to which all stream surfaces converge. Ferri also introduced, for the case of the slightly yawed cone, the concept of the "vortical layer" through which the entropy changes from its constant value on the surface of the cone to the value predicted by Stone's theory and gave a method for correcting Stone's first order solution near the cone surface. Stone's solution however, is valid through most of the flow field between the shock and cone surface. Also, it has been pointed out by Roberts and Riley (Ref. 8)and Woods (Ref. 1) that although the entropy corrections set out by Ferri are logically necessary they may be neglected in practice. It has been found that though Stone's theory was originally intended to be applicable to cases of small yaw, its use for comparatively large values of yaw give reasonably satisfactory results.

In the course of his investigation of the supersonic flow around a yawed cone Woods observed (Ref. 1) that Stone's first order theory broke down in predicting the entropy behind the shock at remarkably low values of yaw. He found that this theory used in conjunction with the M.I.T. cone tables predicts for certain cases a decrease in entropy through the shock wave, which is a phenomenon physically impossible. This aspect of Stone's theory does not seem to have been noticed prior to Wood's work.

From the above considerations it becomes obvious that although Stone's theory is quite satisfactory in respect of many practical applications, a correct and complete solution of the supersonic flow around a yawed cone has not yet been achieved.

The present investigation was carried out in order to make an effort to understand the problem better. One of the assumptions of Stone's theory is that when the cone is yawed, the shock wave continues to be conical [*] with the same semi apex angle as in the non-yaw case; the only difference being that now the shock cone axis will be yawed with respect to the axis of the conical body also. The present investigation was intended to demonstrate how far this assumption was justified by considering the exact flow behind a yawed conical shock wave. The problem essentially consists of positioning a conical shock wave with its axis inclined to the free stream and then investigating the flow behind the shock cone in order to determine the solid body which would produce this particular configuration.

In the present case this is achieved by using a numerical procedure for solving the differential equations of motion, which are set out in Section2. The procedure adopted for the numerical solution and results of the application of this procedure to a particular case is set out in Section 3. A discussion of this solution follows in Section 4.

A comparison between the body shape obtained by the solution of this particular case and the corresponding first order yawed cone solution is made in Figure 15.

---

[*] The terms "conical body" and "Conical shockwave" will be used to indicate respectively bodies and shockwaves of circular cross sections.

2. PROPERTIES OF THE FLOW

2.1. System of Co-ordinates and Nomenclature

We employ spherical polar co-ordinates r, ψ, ω based on the apex of the conical shock wave as origin and the axis of the shock wave coinciding with the axis of the co-ordinate system $\psi = 0$. The plane of yaw (or symmetry) is defined by $\omega = 0$ $\omega = \pi$. A diagram of the co-ordinate system is given in Figure 1. u, v, w are the components of the velocity and they are defined to be positive in the direction r increasing, ψ increasing and ω increasing respectively. The free stream of velocity V_1 is considered to be inclined to the shock axis at an angle α such that the part of the plane of symmetry defined by $\omega = 0$ is on the "leeward" side and $\omega = \pi$ on the "windward" side.

2.2. Conical Flow

In a steady supersonic conical field of flow no fundamental length is involved and the physical properties of the flow are functions only of angular variables. The equations of motion are independent of r.

2.3. Differential equations of motion.

The steady "conical" flow of an inviscid compressible gas with constant specific heat and with no heat conduction satisfies the following equations.

Euler's Equations can be expressed as

$$v \frac{\partial u}{\partial \psi} + \frac{w}{\sin \psi} \frac{\partial u}{\partial \omega} - v^2 - w^2 = 0 \qquad (1)$$

$$- u \frac{\partial u}{\partial \psi} - w \frac{\partial w}{\partial \psi} + \frac{w}{\sin \psi} \frac{\partial v}{\partial \omega} + uv - w^2 \cot \psi = T \frac{\partial S}{\partial \psi} \qquad (2)$$

$$v \sin \psi \frac{\partial w}{\partial \psi} - u \frac{\partial u}{\partial \omega} - v \frac{\partial v}{\partial \omega} + u w \sin \psi + v w \cos \psi = T \frac{\partial S}{\partial \omega} \qquad (3)$$

where S = Entropy T = Temperature.

Equation of Continuity

$$u(v^2 + w^2 - 2a^2) - a^2 v \cot \psi + \frac{\partial v}{\partial \psi}(v^2 - a^2)$$

$$+ \frac{1}{\sin \psi} \frac{\partial w}{\partial \omega}(w^2 - a^2) + v w \left(\frac{\partial w}{\partial \psi} + \frac{1}{\sin \psi} \frac{\partial u}{\partial \omega} \right) = 0 \qquad (4)$$

where a = speed of sound.

It is convenient to combine equations (1), (2) and (3) to give

$$v \frac{\partial S}{\partial \psi} + \frac{w}{\sin\psi} \frac{\partial S}{\partial \omega} = 0 \qquad (5)$$

Equation of Energy

$$C_p T + \frac{q^2}{2} = \text{constant} \qquad (6)$$

where $q^2 = u^2 + v^2 + w^2$

C_p = specific heat at constant pressure

Equation (5) is general for any conical flow and in fact defines the lines of constant entropy which correspond to the streamlines. If L is the streamline projection on the sphere r = constant,

$$\frac{dS}{dL} = \frac{\partial S}{\partial \psi} \frac{d\psi}{dL} + \frac{\partial S}{\partial \omega} \frac{d\omega}{dL} = 0.$$

Using equation (5) we have

$$\left(\frac{d\omega}{d\psi}\right)_L = \frac{w}{v \sin\psi} \qquad (7)$$

2.4. Conical flow without axial symmetry

In reference 9 Ferri has discussed in detail the properties of supersonic conical flow without axial symmetry and has shown that singularities must exist in any such flow. He considers a conical body placed in a free stream inclined to its axis and by physical reasoning shows that the entropy must be constant on the surface of the cone or must change in a discontinuous manner. It has been shown by Ferri that such a discontinuity occurs along the generator of the cone on the "leeward" meridian plane ($\omega = 0$) at which the entropy is many valued. The character of the flow is such that stream lines downstream of the shock cone curve round and converge to this singular generator. The entropy on the cone surface is equal to that on the "windward" meridian plane ($\omega = \pi$).

3. METHOD OF SOLUTION

3.1. Procedure for numerical solution

The differential equations of motion set out in paragraph 2.3 can be integrated step-by-step with respect to ψ making use of numerical differentiation to obtain derivatives with respect to ω. The method in brief, is as follows: Consider the circle of intersection ($\psi = \psi_w$) of the shock cone and sphere r = constant. Choose a large number of azimuthal stations around this circle. The quantities u, v, w, S and T and their derivatives with respect to ω are known on this circle from the shock wave equations. Substituting these values

in the equations we obtain the values of the derivatives with respect to ψ at each azimuthal station. Now consider a small inward step $\Delta\psi$ in ψ (along the sphere r = constant). Making use of numerical integration we obtain values of u, v, w, S and T on the circle $\psi = \psi_w - \Delta\psi$. Derivatives of u, v, w, S and T with respect to ω can be found by numerical differentiation around this circle making use of the values at the various azimuthal stations. Now the derivatives with respect to ψ can be found by substitution in the equations of motion. The process followed above is repeated to carry on the integration as far as is required Details of the procedure adopted are given in Appendix A.

3.2. Accuracy of Method

The accuracy of the method depends mainly on two factors. The first is the choice of the interval between azimuthal stations. The accuracy of the process of numerical differentiation which has to be used to determine the derivatives with respect to ω at each step in ψ depends mostly on the interval between the stations used in the differentiation: the smaller the interval, the more accurate the method will be.

The second factor is the magnitude of $\Delta\psi$ which is chosen for the step-by-step integration The accuracy of the method will be enhanced by using as small a step in ψ as is possible. By a suitable choice of $\Delta\psi$ and use of the process of successive approximations described in Appendix A it is possible to obtain a satisfactory accuracy. In general, the choice of $\Delta\psi$ should be consistent with the choice of the interval between azimuthal stations.

3.3. Details of the solution for a particular case.

The numerical procedure was applied to a particular case with the following initial conditions: Free stream Mach No. $M_1 = 10$ Shock wave semi-apex angle $\psi_w = 30^\circ$ Angle of yaw $\alpha = 20^\circ$.

Eleven azimuthal stations at intervals of 15° were chosen between $\omega = 0$ and $\omega = \pi$ around the shock cone. It was thought that this choice of the interval in ω would give satisfactory results.

Numerical differentiation formulae given by Bickley (Ref.10) were used. Since the derivatives of u, v, w and S with respect to ω could be obtained analytically on the shock wave itself, it provided a check on the accuracy of the numerical differentiation at the start of the solution. Five-point and seven-point formulae were tried along with a central difference formula using up to 7th differences. It was found that the 5-point formula was quite satisfactory in all cases though the 7-point formula was found to be more accurate in the case of $\frac{\partial S}{\partial \omega}$.

Hence, the 5-point formula was used for finding $\frac{\partial u}{\partial \omega}$, $\frac{\partial v}{\partial \omega}$, $\frac{\partial w}{\partial \omega}$ and the 7-point formula for $\frac{\partial S}{\partial \omega}$. In all cases, for finding the derivative at any point an equal number of points on either side of the point were chosen and differentiation formula for the derivative at the middle ordinate were used, since this involved the minimum of error. This procedure could be applied even to points near $\omega = 0$ and $\omega = \pi$ by virtue of the symmetry of the flow about the plane $\omega = 0$, $\omega = \pi$.

Commencing at the shock wave the step-by-step procedure of ψ -wise numerical integration as detailed in Appendix A was carried out using increments $\Delta\psi = 0^{\circ}30'$. It was found that differences between the first approximations and second approximations obtained by invoking the trapezoidal rule were not of great significance (the differences were, in the case of velocities much less than 0.1% and entropy, less than1%) and hence no attempt was made to obtain further approximations.

The same procedure was repeated using increments of $\Delta\psi = 1^{\circ}$ and this gives values which were found to agree very closely with those obtained using half this increment. Thus it was observed that 1° ψ -wise increments would be quite satisfactory.

The solution of the equations proceeded in a very satisfactory manner till a value of $\psi = 26^{\circ}30'$ was reached. At this stage it was observed that 'v' on the "leeward" meridian plane $\omega = 0$ had reached a value very nearly zero and that any further step would take the solutions on this plane beyond the singular point discussed in the previous section. It was also clear that with further steps 'v' would reach zero at other azimuthal stations on the "leeward" side. Hence the solution in the neighbourhood of $\omega = 0$ and beyond $\psi = 26^{\circ}30'$ was difficult to obtain.

It was observed that when v tended to zero the derivatives with respect to ψ changed in magnitude rapidly. This was particularly true about $\frac{\partial w}{\partial \psi}$ and $\frac{\partial S}{\partial \psi}$. This rapid increase in the value of $\frac{\partial w}{\partial \psi}$ seemed to indicate reversals in the azimuthal component of velocity w for the small increment of $\Delta\psi = 0^{\circ}30'$ from beyond $\psi = 26^{\circ}30'$ in the neighbourhood of $\omega = 0$.

Hence as a first step, azimuthal stations were omitted at which large magnitudes of $\frac{\partial w}{\partial \psi}$ indicated reversals in the sign of w, and the solution was carried on for the rest of the stations in steps of $\Delta\psi = 1^{\circ}$. By proceeding in this manner it was possible to continue the process until stages of ψ were reached at which the values of entropy at each azimuthal station (from $\omega = 45^{\circ}$ to $\omega = 180^{\circ}$) had reached the magnitude of the entropy on the meridian plane $\omega = \pi$, thereby indicating the surface of the hypothetical body. The point at which v became zero in the plane $\omega = \pi$ located the position of the intersection of the solid

surface with that plane. This follows from the boundary condition that the velocity component normal to the surface should be zero. On the plane $\omega = 0$, $\omega = \pi$ 'v' is, by symmetry, the normal component of velocity.

To obtain some knowledge about the region between $\omega = 0$ and $\omega = 45^\circ$ beyond $\psi = 26^\circ 30'$, the solution was started again from $\psi = 26^\circ 30'$ using only the five stations at $\omega = 0, 25^\circ, 30^\circ, 45^\circ, 60^\circ$. The integration procedure was repeated using increments of $\Delta\psi = 0^\circ 15'$. During this investigation it was observed that the indication of reversal in sign of w found earlier were due to the choice of increments of ψ and that it was possible to continue the solution without meeting this difficulty by proceeding in very small steps in ψ. This, as mentioned above, was undertaken and this set of calculations gave reasonable results. It was found that the values at $\omega = 45^\circ$ and $\omega = 60^\circ$ obtained in this latter calculation were in agreement with those obtained earlier.

The variation of entropy, temperature and the three velocity components behind the yawed conical shock is presented in the following Figures. Non-dimensional values of u, v, w, S and T as set out in Appendix A are used.

Fig. 7 :- $S \sim \psi$ for various ω.

Fig. 8 :- $S \sim \omega$ for various ψ.

Fig. 9 :- $T \sim \psi$ for various ω.

Fig.10 :- $T \sim \omega$ for various ψ.

Fig.11 :- $u \sim \omega$ for various ψ.

Fig.12 :- $v \sim \omega$ for various ψ.

Fig.13 :- $w \sim \omega$ for various ψ.

By cross plotting from the above figures the projections of constant value lines on a sphere with centre at the origin of the co-ordinate system (apex of shock cone) and radius r = constant were obtained and are shown in the following figures.

Fig. 2 :- Lines of constant entropy (i.e. streamlines)

Fig. 3 :- Lines of constant temperature.

Fig. 4 :- Lines of constant u.

Fig. 5 :- Lines of constant v.

Fig. 6 :- Lines of constant w.

From Fig. 2 we get the shape of the body surface which is defined by S = 1.307.

Having obtained the body shape, the distribution of pressure on the surface could be found. The values of C_p, the pressure coefficient, at the various azimuthal stations around the body surface are compared with the values just behind the shock in Fig. 14.

The head lift and drag coefficient of the body as defined in Appendix B have been calculated.

The lift coefficient $C_L = 0.410$

The drag coefficient $C_D = 0.545$

4. DISCUSSION

4.1. Method of Solution.

As mentioned earlier, the numerical procedure was found to work in a very satisfactory manner up to $\psi = 26^{\circ}30'$, when the solution was in the neighbourbood of the singular point in the "leeward" meridian plane $\omega = 0$. The main difficulty from this stage onwards was that the value of v tended towards zero and a subsequent change in sign (the change in v itself was quite regular throughout). This factor was highly critical since the evaluation of $\frac{\partial u}{\partial \psi}$, $\frac{\partial w}{\partial \psi}$ and $\frac{\partial S}{\partial \psi}$ involved division by v. This meant that whilst the value of v passed through zero and changed sign, it was possible to get large magnitudes of the above derivatives changing in sign quite rapidly. However, this was found to be highly critical only in the case of the evaluation of $\frac{\partial w}{\partial \psi}$. It was this feature which was responsible for the extreme care necessary to continue the solution beyond $\psi = 26^{\circ}30'$ in the vicinity of $\omega = 0$.

As mentioned earlier, this highly critical region between $\omega = 0$ and (as it turned out) $\omega = 45^{\circ}$ was investigated separately using smaller values of $\Delta\psi$ than that used for the remainder of the azimuthal stations. Here it may be mentioned that the above stated difficulties encountered when $v \longrightarrow 0$ and changes sign, were avoided in the case of the "windward" side. This was because the surface of the solid body (as represented by the line of constant entropy of magnitude equal to that of the entropy on the "windward" plane $\omega = \pi$) was obtained before the critical region ($v \longrightarrow 0$) was reached. The solution was not carried any further because the behaviour of the flow inside the body surface was of no special interest in the present case.

4.2. Properties of the flow.

4.2.1. Velocity.

It is found that the variation of the velocity components is quite regular and exhibit no peculiarities. However, the variation in the values of u and particularly w in the vicinity of the singular point needs some consideration. Some difficulty was experienced in the finding of the numerical values of w and u in the region $60^{\circ} > \omega > 0^{\circ}$ for values of ψ smaller than $26^{\circ}30'$. Although it appeared that the values of u and w behaved regularly in this region it was considered that accurate numerical values could only be obtained if smaller intervals of ω were used in the numerical method.

The component v is found to vary in a very regular manner. This is quite understandable since the evaluation of $\frac{\partial v}{\partial \psi}$ depends on $(v^2 - a^2)$ with $v^2 \ll a^2$.

4.2.2. Temperature.

The variation of temperature follows from the way in which the velocity changes. It is found that the variation in temperature throughout the field is quite regular.

4.2.3. Entropy and streamlines.

The distribution of entropy in the flow behind the shock cone is represented in Fig. 2, 7, 8. The projections of constant entropy lines (they correspond to streamlines) on the sphere r = constant are represented in Fig. 2. The location of the singular point, on the "leeward" meridian plane $\omega = 0$, at which the entropy is many valued is also indicated in the figure. It is found that the streamlines, after leaving the shock cone, curve round and converge to the singular point. The surface of the hypothetical solid body (corresponding to the constant entropy line having the same entropy as a plane $\omega = \pi$) which will produce the shock wave dealt with here is also indicated in the figure.

One feature in the pattern of the streamlines near the singular point may be pointed out. From equation (5) we have

$$v \frac{\partial S}{\partial \psi} + \frac{w}{\sin \psi} \frac{\partial S}{\partial \omega} = 0 \quad \text{from which we have as equ.(7)}$$

$$\left(\frac{d \omega}{d \psi}\right)_{\text{streamline}} = \frac{w}{v \sin \psi}$$

or more conveniently

$$\left(\frac{d \psi}{d \omega}\right)_{\text{streamline}} = \frac{v \sin \psi}{w}$$

Except in the meridian plane when v = 0 (and when w = 0) the equation is indeterminate, the above equation holds good generally. Hence, when $v \to 0$ and changes sign (but $w \neq 0$) the streamlines will tend to "flatten" out and become parallel to the line ψ = constant at v = 0 and then "curl up" when v becomes positive. This is illustrated in the accompanying diagram.

This happened in the case of a few streamlines on the "leeward" side.

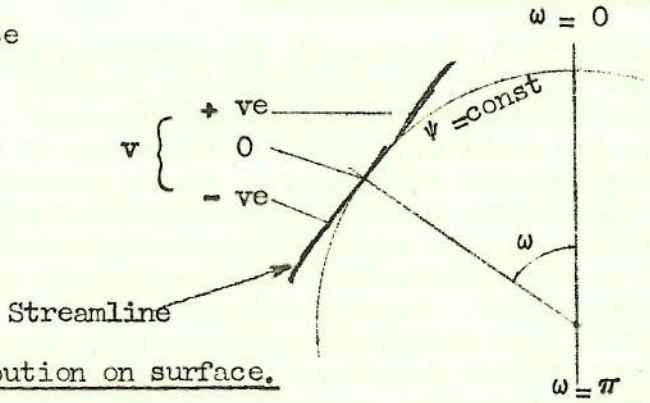

4.2.4. Pressure distribution on surface.

The pressure distribution on the body was worked out and a comparison with the values on the downstream side of the shock wave is made in Fig.14. This indicates that there is an expansion in the flow between the shock wave and body except in a small region ω = 140 to 180° on the "windward" side where a slight compression of the flow takes place.

4.2.5. Comparison with first order solution.

The body shape obtained by the present method is compared here with the first order yawed cone solution (Ref.2.6) in Fig. 15. It is observed that the body is smaller than the corresponding cone in the fist order solution. The body is not wholly circular; however, it is noted that it is mostly circular with a small hump on the "leeward" side. The smaller size of the body as noted in the case of the present solution might mean that in actual practice the assumption of the first order theory at comparatively large yaw with respect to shape of the shock cone may be valid but that it may be necessary to make a correction for the change in size of the shock cone.

The head lift and drag coefficients of the conical body (of non-circular cross section) obtained by the present method have been calculated using expressions defined in Appendix B.

Head lift coefficient $C_L = 0.410$

and a Head drag coefficient $C_D = 0.545$

These first order values were obtained only as a means of checking the orders of magnitude of C_L and C_D obtained for the body of the present solution. A direct comparison between the two sets of values cannot be considered to have any conclusive significance.

4.3. Method of numerical solution.

It is felt that, in general, the numerical investigation was satisfactory. However, the difficulties involved in carrying on the solution near the singular point on the "leeward" side have shown that extreme care has to be exercised in the choice of the interval between azimuthal stations and steps in ψ. In the present investigation the region between $\omega = 0$ and $\omega = 45$ was studied separately by carrying out the solution at five equispaced azimuthal stations. It is felt that this is not a very satisfactory method and could be improved upon to a considerable extent. For investigation of the flow in this region it is necessary to have azimuthal stations closer to each other than 15°. It may perhaps be best to choose a larger number of azimuthal stations on the "leeward" side than on the "windward" side. For future work it is suggested that azimuthal stations should be spaced at intervals of $\Delta\omega = 5^\circ$ from $\omega = 0$ to $\omega = 75$ and at intervals of 15° from $\omega = 75$ to $\omega = 180^\circ$.

5. CONCLUSIONS

It has been found that the numerical method adopted for the investigation of the exact flow behind a yawed conical shock is simple to use and produced reasonably satisfactory results. The accuracy of the method can be improved by choosing a smaller interval between azimuthal stations.

As a particular case, the flow behind a conical shock of semi-apex angle 30° inclined at 20° to a free stream of Mach Number 10 has been investigated and the shape of the conical body (of non-circular section) which would produce such a shock wave has been determined and compared with the yawed cone solution. In this case, it has been found that the shape departs from circular only to a small extent on the "leeward" side. More significantly, it is noted that the size of the body is smaller than that of the circular cone which according to Stone's first order theory (Ref.2,6) would produce the given shock wave.

The properties of the flow between the shock cone and the solid body surface have been determined and the pattern of the streamlines has been studied. The existence of a singular generator on the body surface in the "leeward" meridian plane $\omega = 0$, at which the entropy is many valued has been well brought out.

6. ACKNOWLEDGEMENTS.

The author acknowledges with gratitude the advice and help given by Mr T.R.F.Nonweiler who suggested the subject of this thesis and supervised the work.

REFERENCES.

1.	Woods, B.A.	The supersonic flow around a yawed cone. College of Aeronautics Thesis, June 1956, (unpublished).
2.	Stone, A.H.	On the supersonic flow past a slightly yawing cone. Journal of Mathematics and Physics, Vol.27. 1948.
3.	Taylor G.I., and Maccoll J.W.	The air pressure on a cone moving at high speeds. Proc. Roy.Soc. Series A, Vol.139, 1933.
4.	Stone, A.H.	On supersonic flow past a slightly yawing cone II. Journal of Mathematics and Physics, Vol.30. 1951.
5.	Kopal,Z and staff of Computing Lab.	Tables of supersonic flow around cones. M.I.T. Report No. 1, 1947.
6.	"	Tables of supersonic flow around yawing cones. M.I.T. Report No. 3, 1947.
7.	"	Tables of supersonic flow around cone of large yaw. M.I.T. Report No. 5, 1949.
8.	Roberts, R.C., and Riley, J.D.	A guide to the use of M.I.T. cone tables. Journal Aero.Sc. Vol.21 May 1954.
9.	Ferri, A.	Supersonic Flow around circular cones at angles of attack. NACA Report 1045 (1951) T.N.2236 (1950).
10.	Bickley,W.G.	Formulae for numerical differentiation. Mathematical Gazette, Vo.25 (1941), p.22.
11.	Ames Research Staff.	Equations, tables and charts for compressible flow. NACA Report 1135.(1953).
12.	Young, G.B.W., and Siska, C.P.	Supersonic flow around cones at large yaw. Journal Aero.Sc. Vol.19 No. 2. Feb. (1952).

APPENDIX A.

DETAILS OF SOLUTION.

A.1. Procedure for numerical solution.

The differential equations of motion (1) to (6) set out in paragraph 2.3 can be expressed in non-dimensional form by effecting the following substitutions. (Primes denote non-dimensional quantities).

$$u' = \frac{u}{V_1} \quad , \quad v' = \frac{v}{V_1} \quad , \quad w = \frac{w}{V_1}$$

$$S' = \frac{S}{C_p} \quad , \quad T' = \frac{T}{V_1^2/C_p} \qquad \text{where } V_1 = \text{free stream velocity}$$

and $$a' = \frac{a}{V_1} \qquad a^2 = (a' V_1)^2 = \alpha R T' \frac{V_1^2}{C_p}$$

$$(a')^2 = (\gamma - 1) T'$$

using the above relations we have

$$v' \frac{\partial u'}{\partial \psi} + \frac{w'}{\sin \psi} \frac{\partial u'}{\partial \omega} - v^2 - w^2 = 0 \qquad (1)A$$

$$- u' \frac{\partial u'}{\partial \psi} - w' \frac{\partial w'}{\partial \psi} + \frac{w'}{\sin \psi} \frac{\partial v'}{\partial \omega} + u' v' - w' \cot \psi = T' \frac{\partial S'}{\partial \psi} \qquad (2)A$$

$$v' \sin \psi \frac{\partial w'}{\partial \psi} - u' \frac{\partial u'}{\partial \omega} - v' \frac{\partial v'}{\partial \omega} + u' w' \sin \psi + v' w' \cos \psi = T' \frac{\partial}{\partial \omega} \frac{S'}{} \qquad (3)A$$

$$u' (v'^2 + w'^2 - 2 [\alpha - 1] T') - (\alpha - 1) T' v' \cot \psi + \frac{\partial v'}{\partial \psi} (v'^2 - [\alpha - 1] T')$$

$$+ \frac{1}{\sin \psi} \frac{\partial w'}{\partial \omega} (w'^2 - [\alpha - 1] T') + v' w' \left(\frac{\partial w'}{\partial \psi} + \frac{1}{\sin \psi} \frac{\partial v'}{\partial \omega} \right) = 0 \qquad (4)A$$

$$v' \frac{\partial S'}{\partial \psi} + \frac{w'}{\sin \psi} \frac{\partial S'}{\partial \omega} = 0 \qquad (5)A$$

$$T' + \frac{q'^2}{2} = \text{constant}$$

$$= T_1' + \frac{V_1'^2}{2} = T_1' + \frac{1}{2} \qquad (6)A$$

Hereafter these non-dimensional quantities will be used and the primes will be omitted.

The above mentioned differential equations can be integrated step-by-step, for small steps in ψ, proceeding inwards from a large number of azimuthal stations on the shock cone defined by various values of ω. The procedure is as follows :

(i) Choose a sufficiently large number of azimuthal stations (preferably equally spaced) around the shock wave from $\omega = 0$ to $\omega = \pi$. Since the flow is symmetrical about the plane of yaw it is sufficient to consider only the region on one side of the plane. The physical properties of the flow just behind the shock wave are known from the shock wave equations. We will use the subscript '2' to indicate conditions just behind the shock wave. (Subscript '1' is used for free stream condition). From the shock wave equations the values of u_2, v_2, w_2, T_2, S_2 and $\frac{\partial u_2}{\partial \omega}$, $\frac{\partial v_2}{\partial \omega}$, $\frac{\partial w_2}{\partial \omega}$, $\frac{\partial S_2}{\partial \omega}$ can be calculated at each azimuthal station. These values can be substituted in equations (1), (3), (4) and (5) (it is sufficient to use either (2) or (4)) to give $\frac{\partial u_2}{\partial \psi}$, $\frac{\partial v_2}{\partial \psi}$, $\frac{\partial w_2}{\partial \psi}$ and $\frac{\partial S_2}{\partial \psi}$.

(ii) Now choose a sufficiently small increment in ψ, $\Delta\psi$ say, and obtain a first approximation to the values of u_3, v_3, w_3, S_3 at $\psi_3 = \psi_2 - \Delta\psi$ at each azimuthal station. This is achieved by the use of the simple point-slope formula which in general terms can be written as

$$y_{n+1} = y_n + hy'_n \quad , \text{ where } y = f(x), \quad y' = \frac{dy}{dx}$$

$$y_{n+1} = f(x_{n+1}), \; y_n = f(x_n)$$

$$h = x_{n+1} - x_n$$

The first approximation to the value of T_3 can be obtained by substituting the values of u_3, v_3, w_3 obtained above in equation (6).

(iii) Having obtained the values of u_3, v_3, w_3, S_3 at the various azimuthal stations for $\psi = \psi_3$, $\frac{\partial u_3}{\partial \omega}$, $\frac{\partial v_3}{\partial \omega}$, $\frac{\partial w_3}{\partial \omega}$, $\frac{\partial S_3}{\partial \omega}$ can be obtained by numerical differentiation.

(iv) Now the differential equations can be used to obtain

$$\frac{\partial u_3}{\partial \psi}, \quad \frac{\partial v_3}{\partial \psi}, \quad \frac{\partial w_3}{\partial \psi}, \quad \frac{\partial S_3}{\partial \psi}$$

and using these values of the derivatives with respect to ψ at ψ_3, and those at ψ_3, the trapezoidal formula

$$y_{n+1} = y_n + \frac{h}{2} (y_{n+1}' + y_n')$$

can be used to give a second approximation to the values of u_3, v_3, w_3 and S_3 at ψ_3. This also provides a check on the numerical accuracy of the first approximation.

(v) The process detailed above can be repeated to give successive approximations to the values at ψ_3 until no changes in the values occur to the accuracy required.

(vi) Having satisfactorily completed the first step (from ψ to ψ_3) a further step can be taken. Consider another increment $\Delta\psi^2$ and obtain a first approximation to the values (of u, v, w, S) at $\psi_4 = \psi_3 - \Delta\psi$ by the more accurate formula

$$y_{n+1} = y_{n-1} + 2 h y_n'.$$

The same procedure which was used for the first step is repeated and the derivatives with respect to ψ at each of the aximuthal stations calculated for $\psi = \psi_4$. The trapezoidal rule can be invoked to give a second approximation to the values at ψ_4. The whole process can be repeated if necessary to give further approximations.

(vii) The same procedure is used to carry the solution forward for as many steps in ψ as is required.

APPENDIX B

CALCULATION OF LIFT AND DRAG COEFFICIENTS.

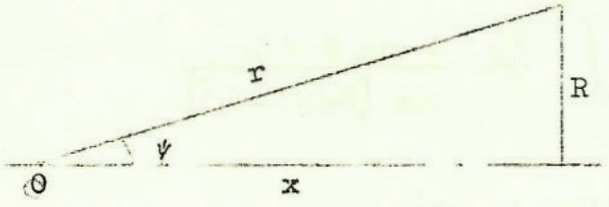

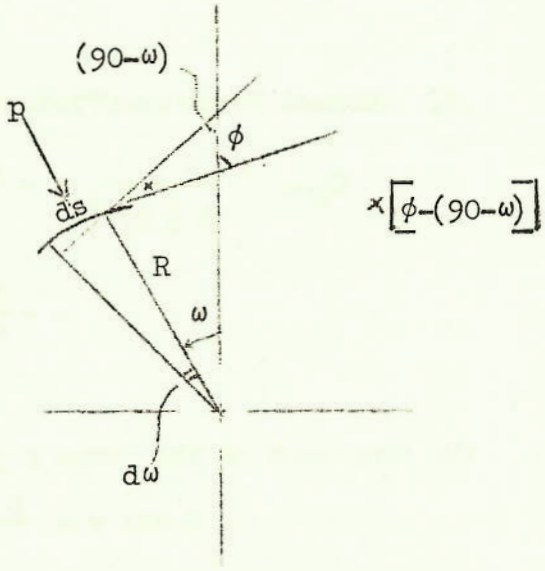

consider a length x of the body (a cone of general cross section) measured from the apex at origin O. We use in addition to the spherical co-ordinates (r, ψ, ω) a cylindrical polar co-ordinate system (x, R, ω) such that $r = x \cos \psi$ and $r = R \sin \psi$. Now consider an elemental length ds along the circumference of the general shaped cross section. Let ds be inclined to the vertical at an angle ϕ. Then

$$ds = \frac{R\, d\, \omega}{\cos\left[\phi-(90-\omega)\right]}$$

Force on (the triangular) elemental area (r, ds)

$$f = \frac{p\, r\, d\, s}{2}$$

component of the above force perpendicular to an axis (i.e. the component force lies in the plane x = constant).

$$= f \cos \psi = \frac{p\, r\, d\, s}{2} \cos \psi = \frac{p\, d\, s}{2}\, x$$

component of this force normal to the axis and parallel to the plane of symmetry $\omega = 0$, $\omega = 180^{\circ}$ is

$$= (f \cos \psi) \sin \phi = \frac{p\, d\, s}{2}\, x \sin \phi.$$

[The components perpendicular to plane of symmetry cancel each other acting from the two sides of the plane.]

∴ Normal force on body length x,

$$N = 2x \int_0^{\pi} \frac{p\, d\, s}{2} \sin\phi = 2x \int_0^{\pi} \frac{(p - p_1)}{2} \sin\phi \, ds, \text{ say}$$

since p_1 is constant,

$\therefore$ Normal Force coefficient

$$C_N = \frac{-N}{A \frac{1}{2} p_1 v_1^2} = -\frac{2x}{A} \int_0^{\pi} \frac{C_p}{2} \sin\phi \, ds \text{ , where A = base area.}$$

$$= -\frac{2x}{A} \int_0^{\pi} \frac{C_p}{2} \frac{R \sin\phi \, d\omega}{\cos\left[\phi - (90 - \omega)\right]}$$

The component of the force f parallel to axis

$$= f \sin\psi = \frac{p\, r\, d\, s}{2} \sin\psi = \frac{p\, d\, s}{2} \, x \tan\psi .$$

Hence we get the

Axial force coefficient

$$C_A = \frac{2x}{A} \int_0^{\pi} \frac{C_p}{2} \frac{R \tan\psi}{\cos\left[\phi - (90 - \omega)\right]} d\omega$$

From the above we have if β is the angle of yaw

Lift coefficient $C_L = C_N \cos\beta - C_A \sin\beta$ (Head Lift Coeff.)

Drag coefficient $C_D = C_A \cos\beta + C_N \sin\beta$ (Head Drag Coeff.)

The coefficients C_N, C_A, C_L and C_D pertain to complete cone from apex to the section considered and do not include base pressures.

Lift and Drag of Equivalent Cone.

The semi-apex angle of a circular cone that will in axi-symmetric flow at $M_1 = 10$, produce a conical shock wave of semi-apex and $\psi_w = 30^\circ$ is $\psi_s = 26.6^\circ$(approx). This was obtained from chart 5 in Ref. 11.

Making use of the 1st order theory of Stone (Ref.2) we have that when the cone is yawed with respect to the free stream (at an angle β) the shock will retain its size and shape but its axis will be inclined to the free stream at an angle (in general not equal to β). From part II of Ref. 6 we have that for $\psi_s = 26.6^\circ$, $M_1 = 10$ (by graphical interpolation) $\frac{\alpha}{\beta} = 1.046$.

$\therefore \beta = 19.1^\circ$. We have further that

$K_N = 0.628$ and $K_D = 0.167$ where K_N and K_D are coefficients of normal and drag forces defined according to wind co-ordinates in Ref. 6. The transformation to the more practical body co-ordinate system can be effected as follows. This method was pointed out by Young and Siska in Reference 12 who give the following formulae for the transformations.

Normal Force Coefficient

$$C_N = \left(\frac{8\beta}{\pi}\right) K_n = \frac{8 \times .333}{\pi} \times .628 = \underline{0.533}$$

$\beta = 19.1^\circ = 0.333$ radians

$\cos\beta = 0.945$

$\sin\beta = 0.327$

Axial Force Coefficient

$$C_A = \frac{8}{\pi} K_D = \frac{8 \times .167}{\pi} = \underline{0.425}$$

$$C_L = C_N \cos\beta - C_A \sin\beta = .504 - .139 = \underline{0.365}$$

$$C_D = C_A \cos\beta + C_N \sin\beta = .402 + .174 = \underline{0.576}$$

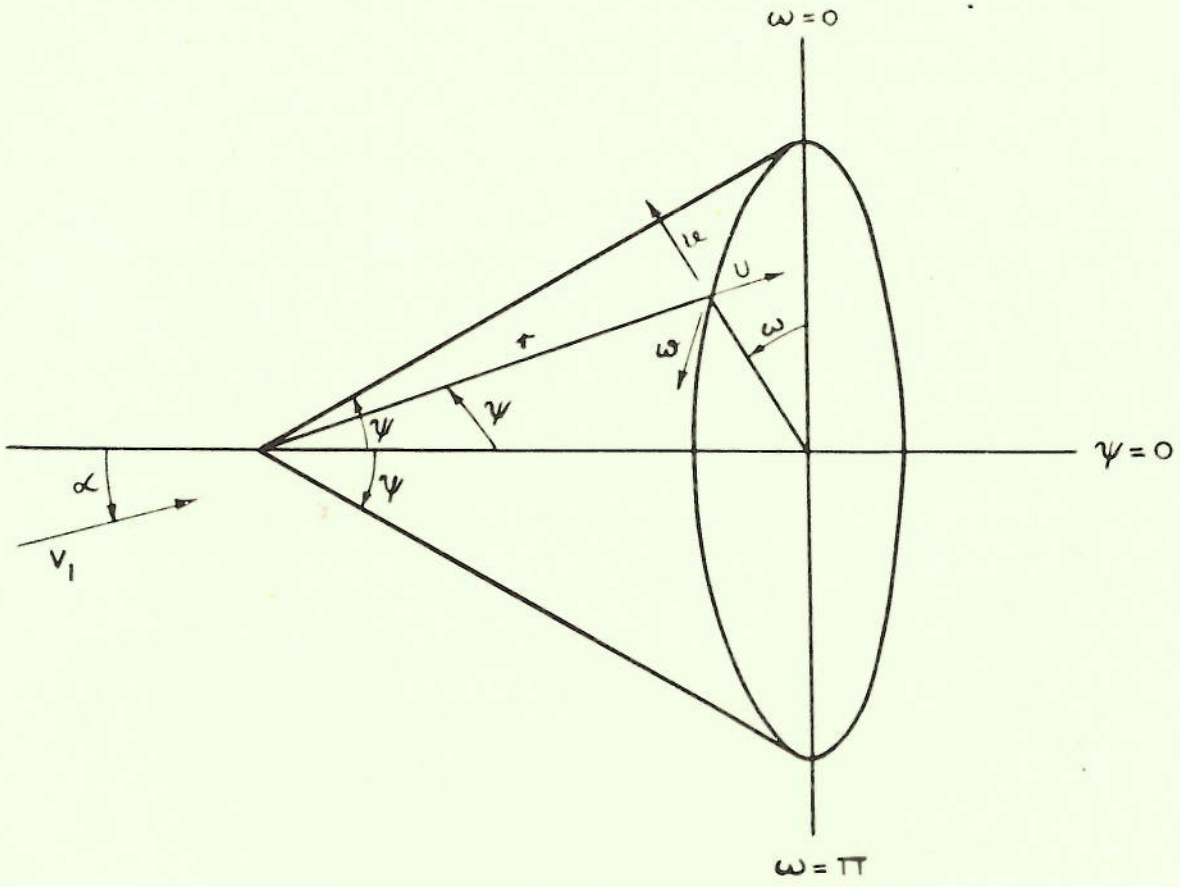

FIG. 1. THE COORDINATE SYSTEM AND NOMENCLATURE

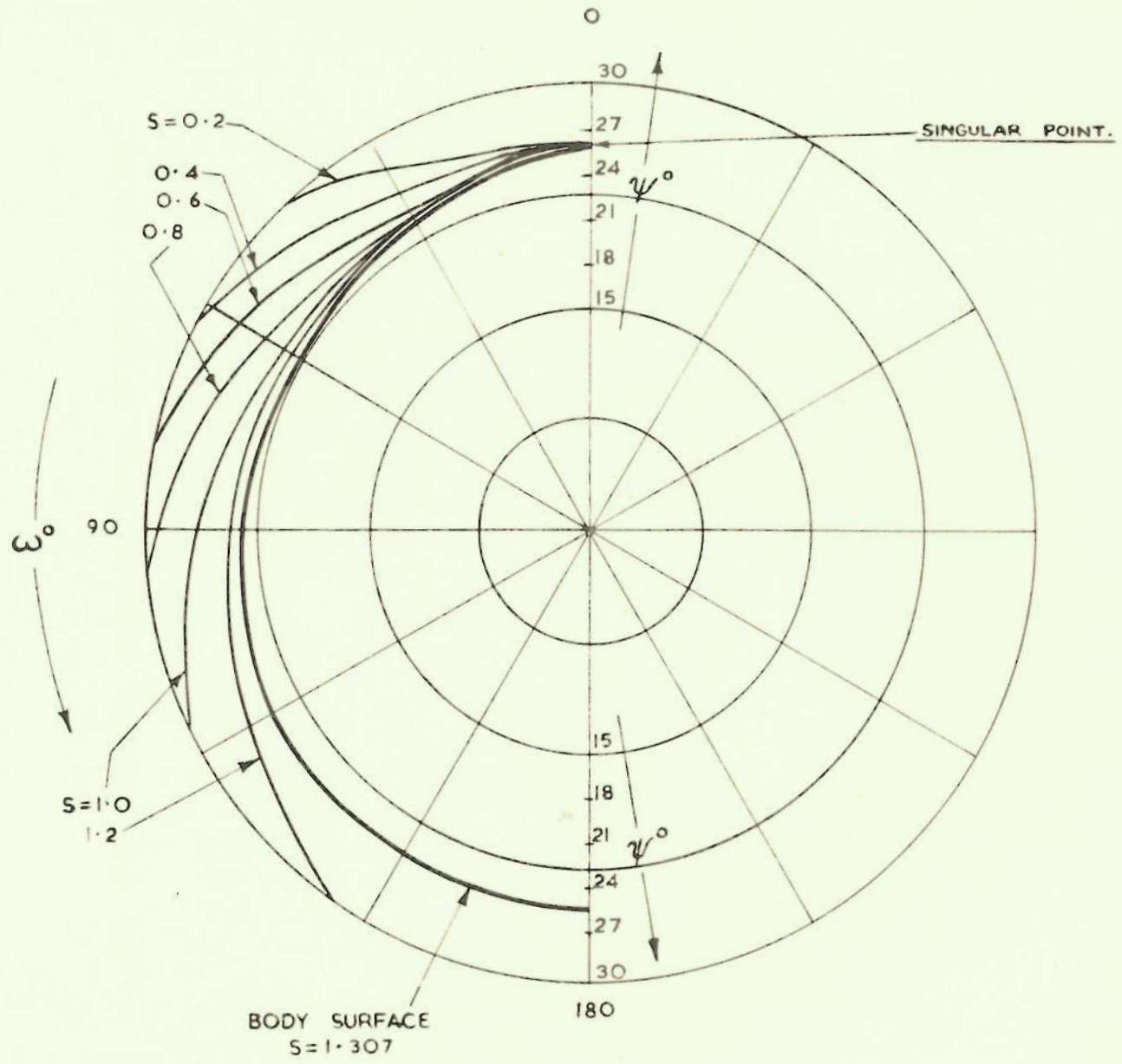

FIG. 2. VARIATION OF ENTROPY BEHIND YAWED CONICAL SHOCK
$M = 10 \quad \psi_w = 30^\circ \quad \alpha = 20^\circ$ LINES OF CONSTANT ENTROPY

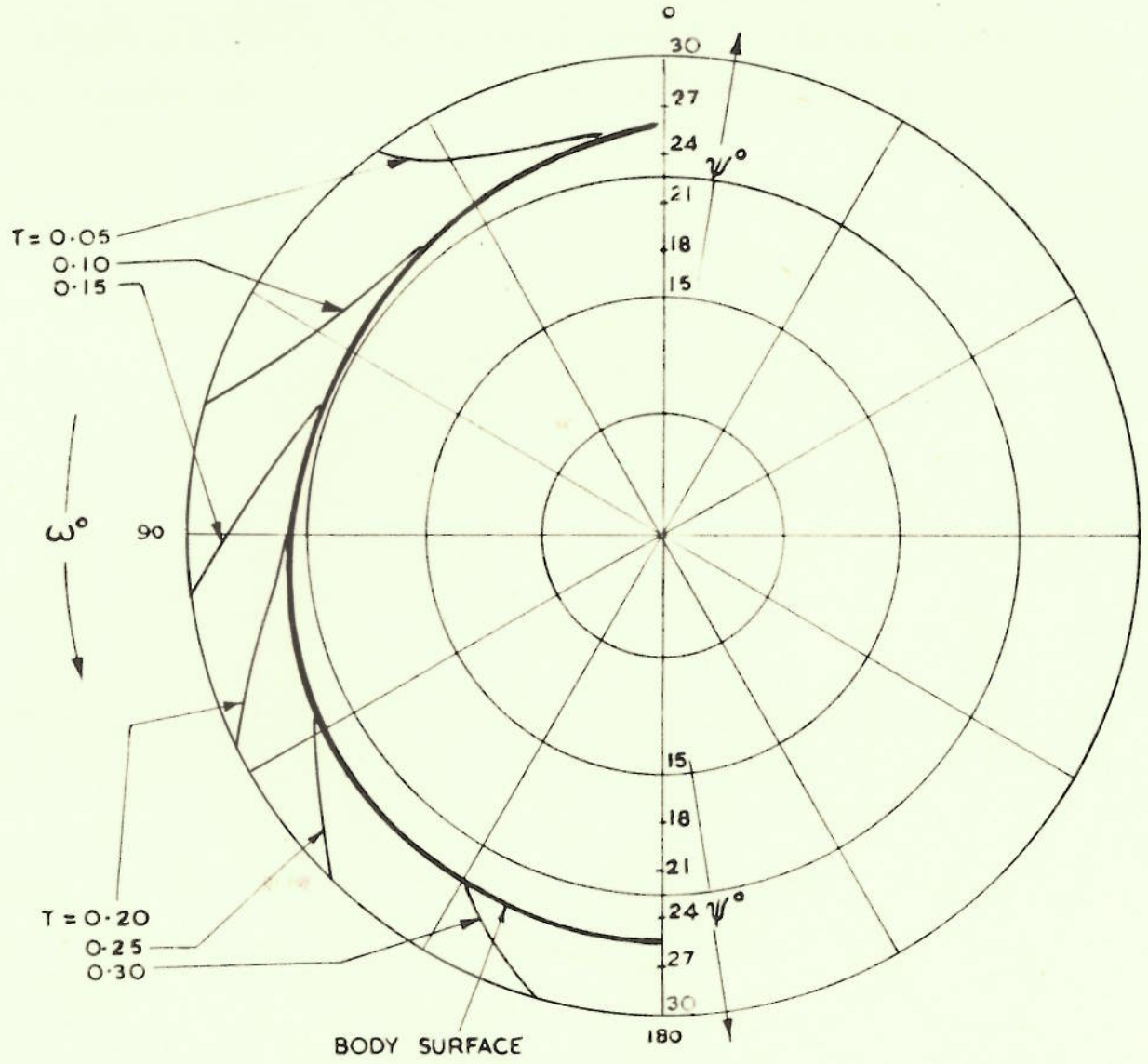

FIG. 3. VARIATION OF TEMPERATURE BEHIND YAWED CONICAL SHOCK
M = 10 $\psi_w = 30^\circ$ $\alpha = 20^\circ$ LINES OF CONSTANT TEMPERATURE

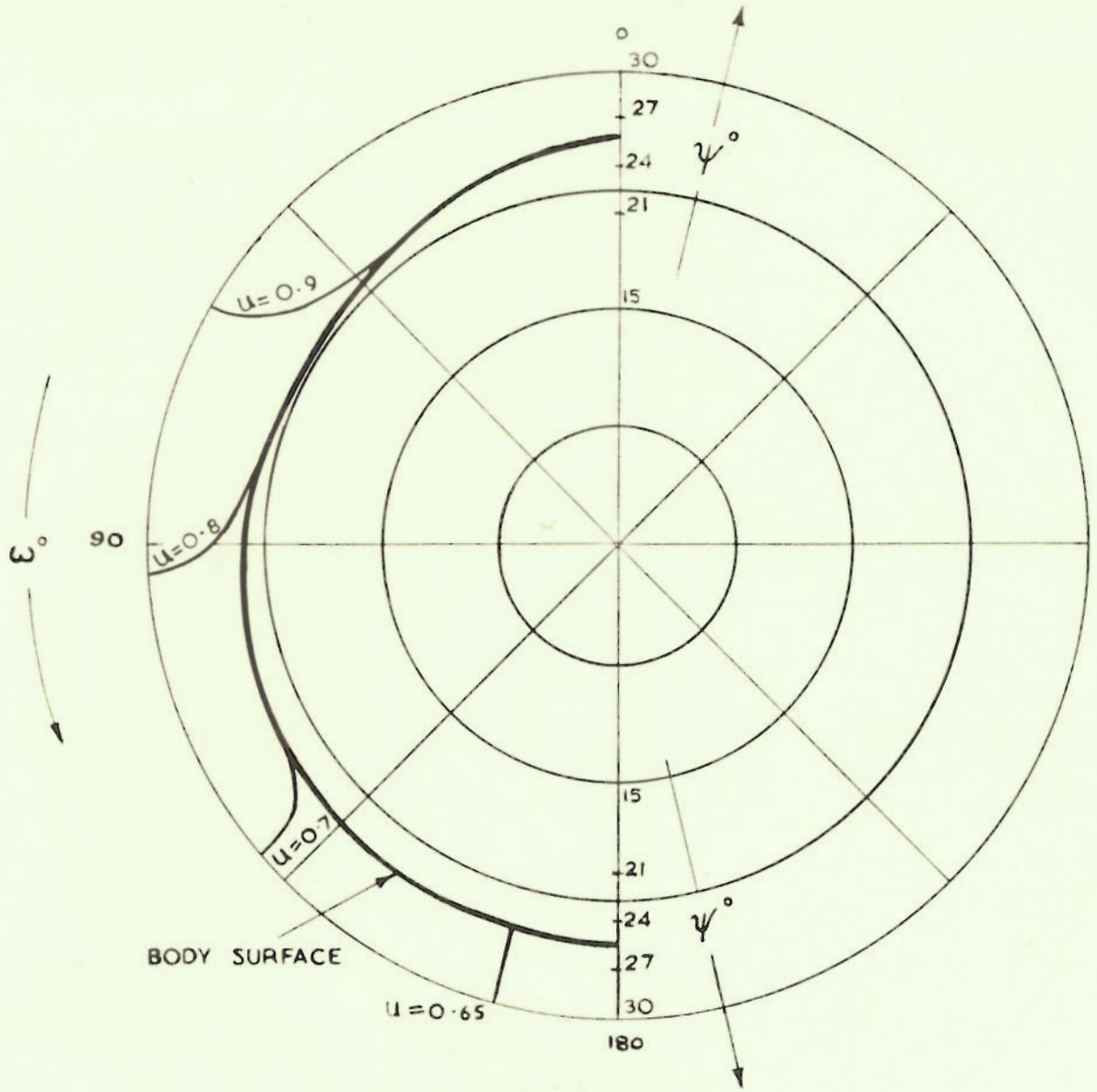

FIG. 4. VARIATION OF u BEHIND YAWED CONICAL SHOCK
M = 10 $\psi_w = 30^\circ$ $\alpha = 20^\circ$ LINES OF CONSTANT u

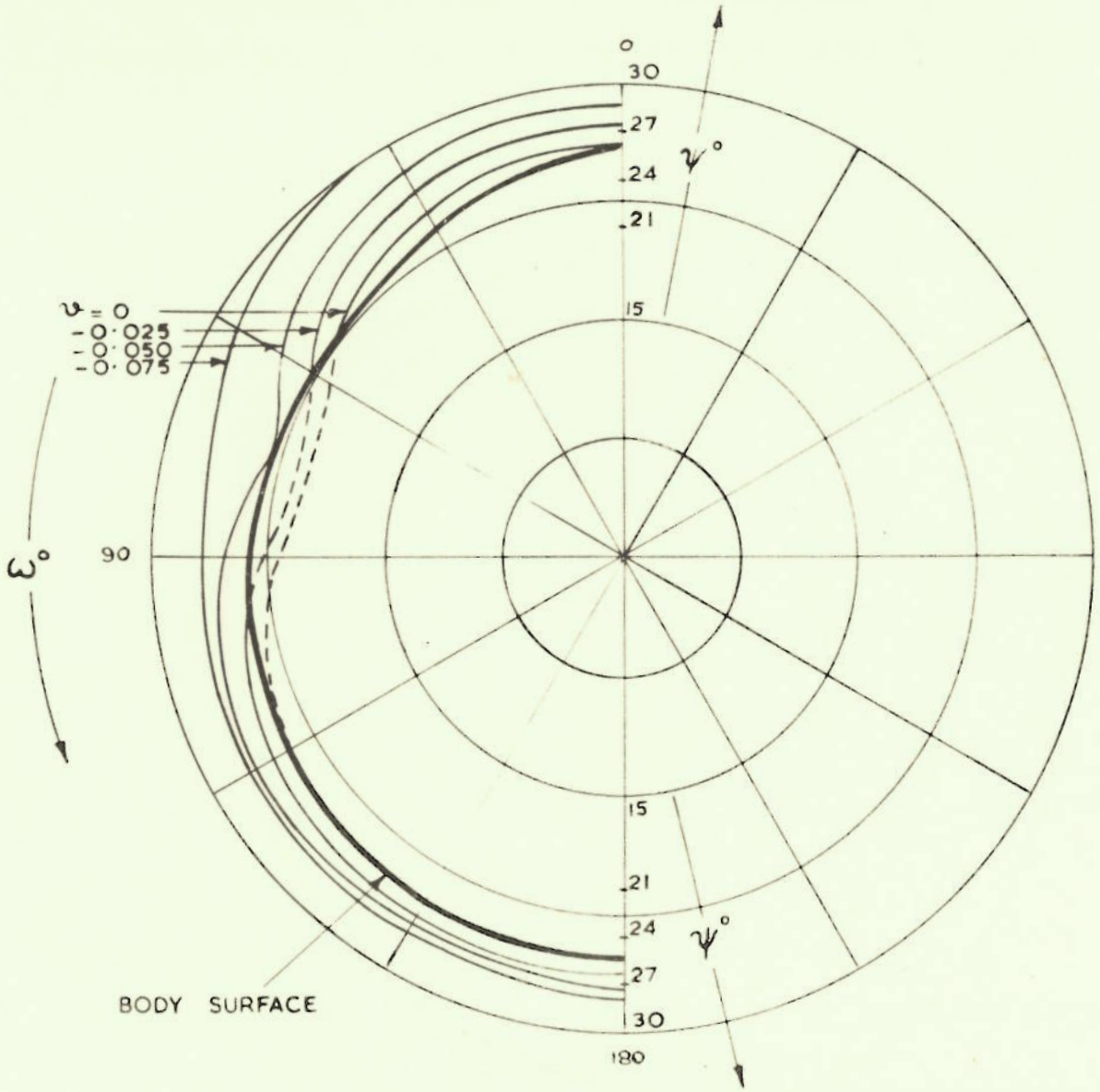

FIG. 5. VARIATION OF υ BEHIND YAWED CONICAL SHOCK
M = 10 $\psi_w = 30^\circ$ $\alpha = 20^\circ$ LINES OF CONSTANT υ

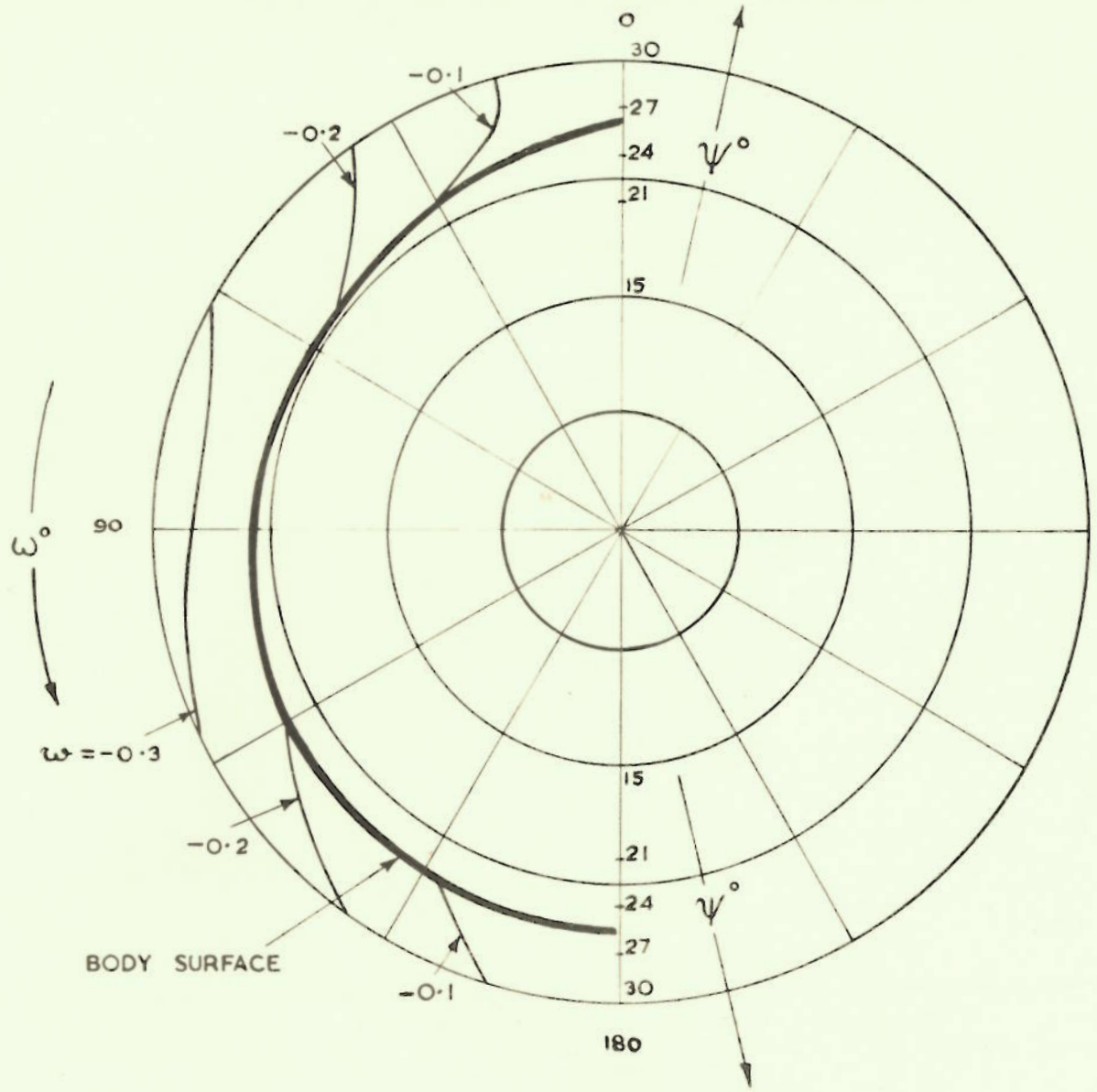

FIG. 6. VARIATION OF ω BEHIND YAWED CONICAL SHOCK

M = 10 $\psi_w = 30^\circ$ $\alpha = 20^\circ$ LINES OF CONSTANT ω

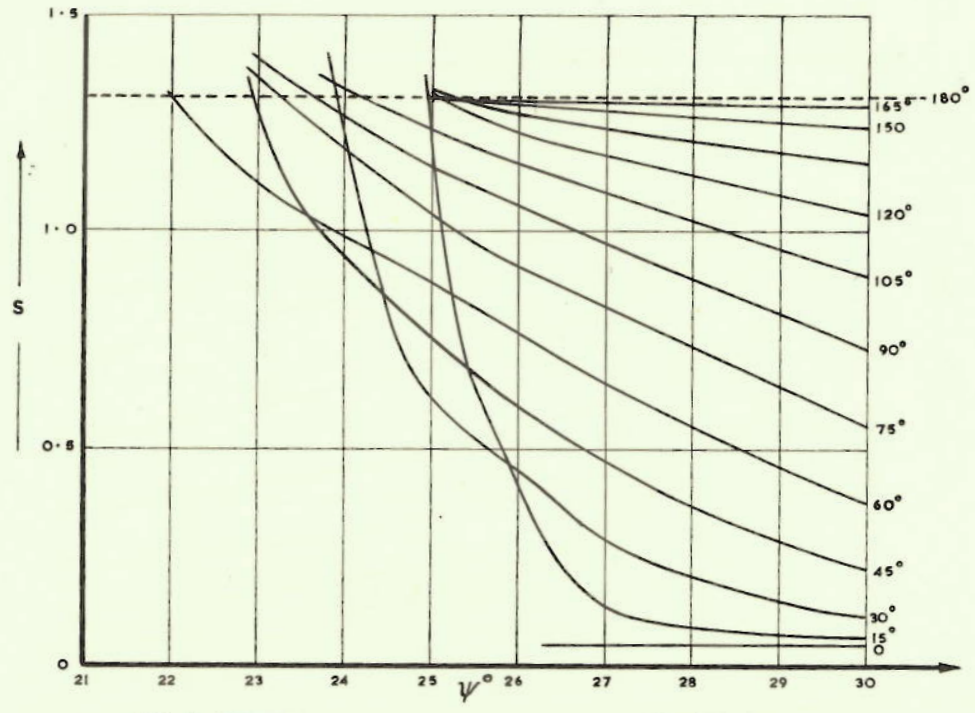

FIG. 7. VARIATION OF ENTROPY BEHIND YAWED CONICAL SHOCK
M = 10 $\psi_w^\circ = 30^\circ$ $\alpha = 20^\circ$ $S \sim \psi$

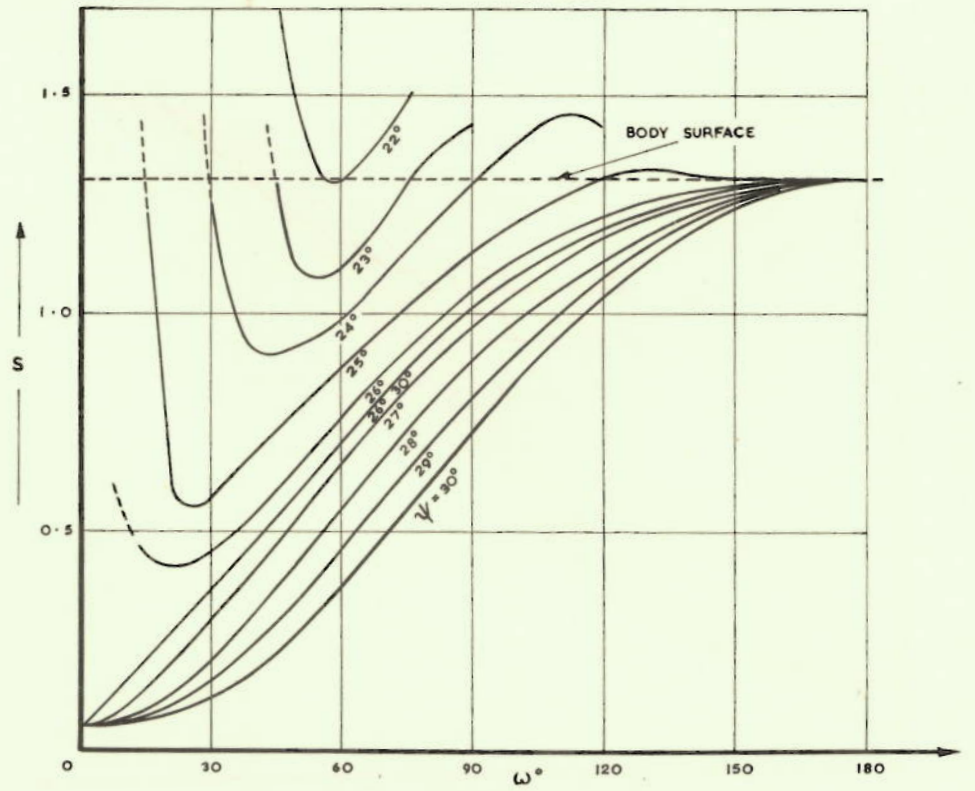

FIG. 8. VARIATION OF ENTROPY BEHIND YAWED CONICAL SHOCK
M=10 $\psi_w = 30^\circ$ $\alpha = 20$ $S \sim \omega$

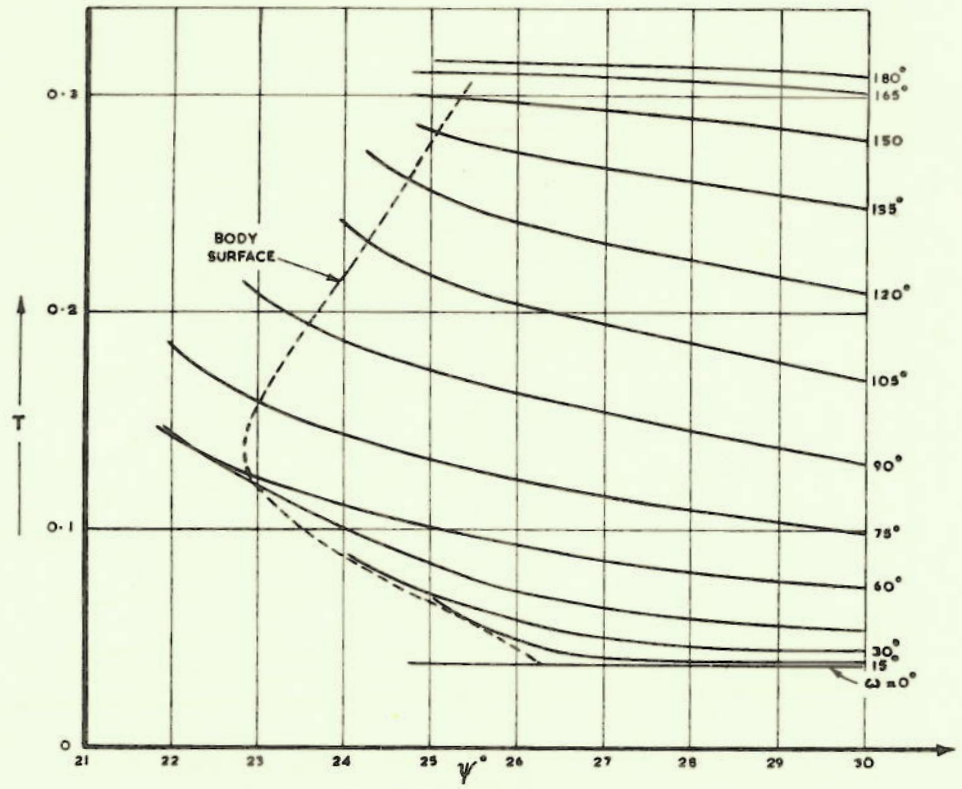

FIG. 9. VARIATION OF TEMPERATURE BEHIND YAWED CONICAL SHOCK
$M = 10 \quad \psi_w = 30^\circ \quad \alpha = 20^\circ \quad T \sim \psi$

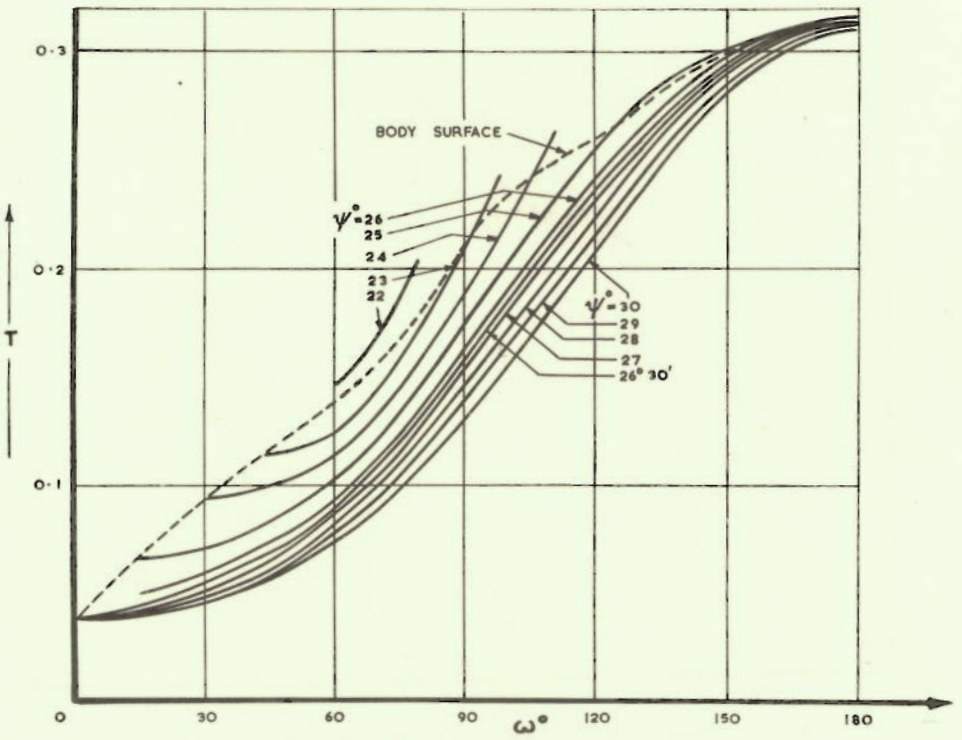

FIG. 10. VARIATION OF TEMPERATURE BEHIND YAWED CONICAL SHOCK
$M = 10 \quad \psi_w = 30^\circ \quad \alpha = 20^\circ \quad T \sim \omega$

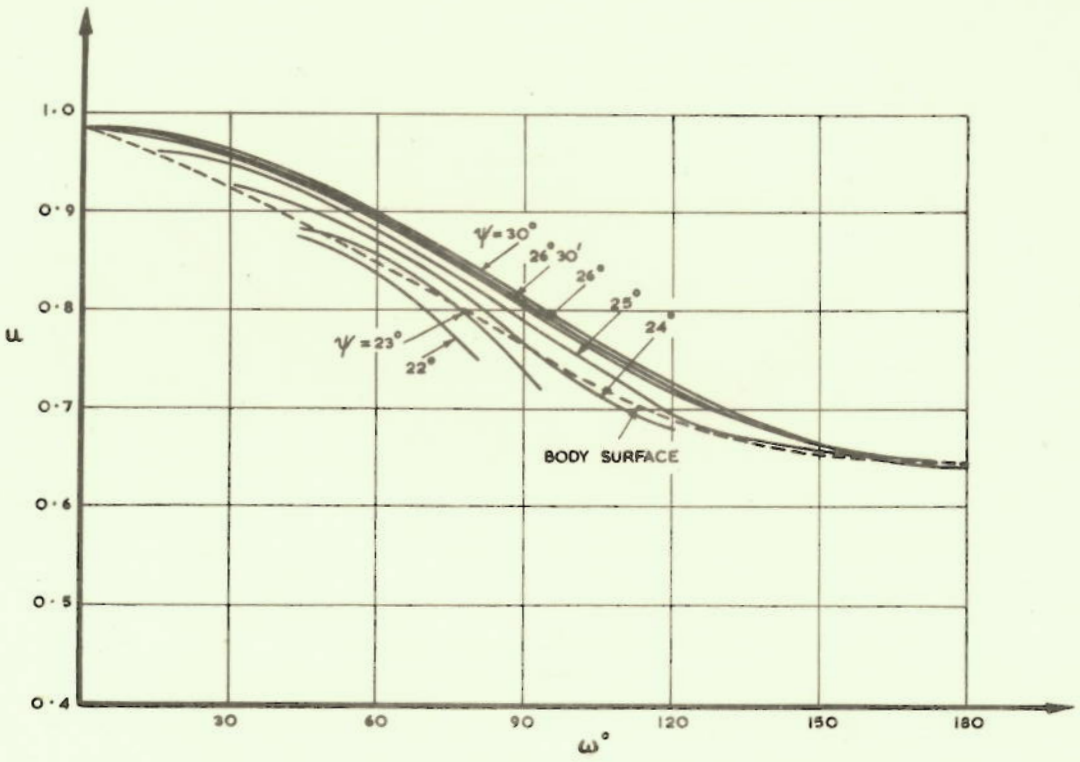

FIG. 11. DISTRIBUTION OF u BEHIND YAWED CONICAL SHOCK
$M=10$ $\psi_w=30^\circ$ $\alpha=20^\circ$ $u \sim \omega$

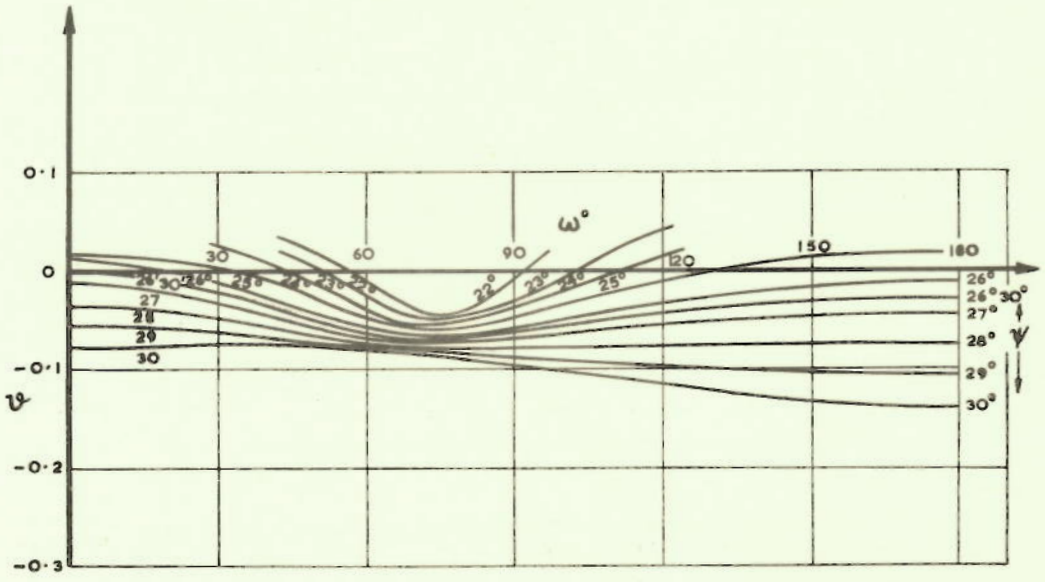

FIG. 12. DISTRIBUTION OF v BEHIND YAWED CONICAL SHOCK
$M=10$. $\psi=30^\circ$ $\alpha=20^\circ$ $v \sim \omega$

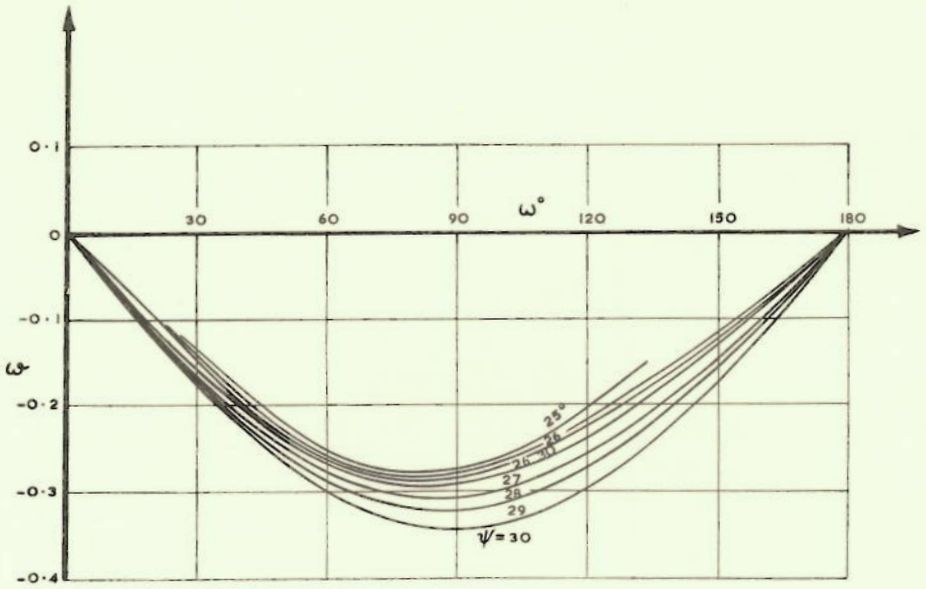

FIG. 13. DISTRIBUTION OF ω BEHIND YAWED CONICAL SHOCK
M = 10 $\Psi = 30^\circ$ $\alpha = 20^\circ$ $\omega \sim \omega$

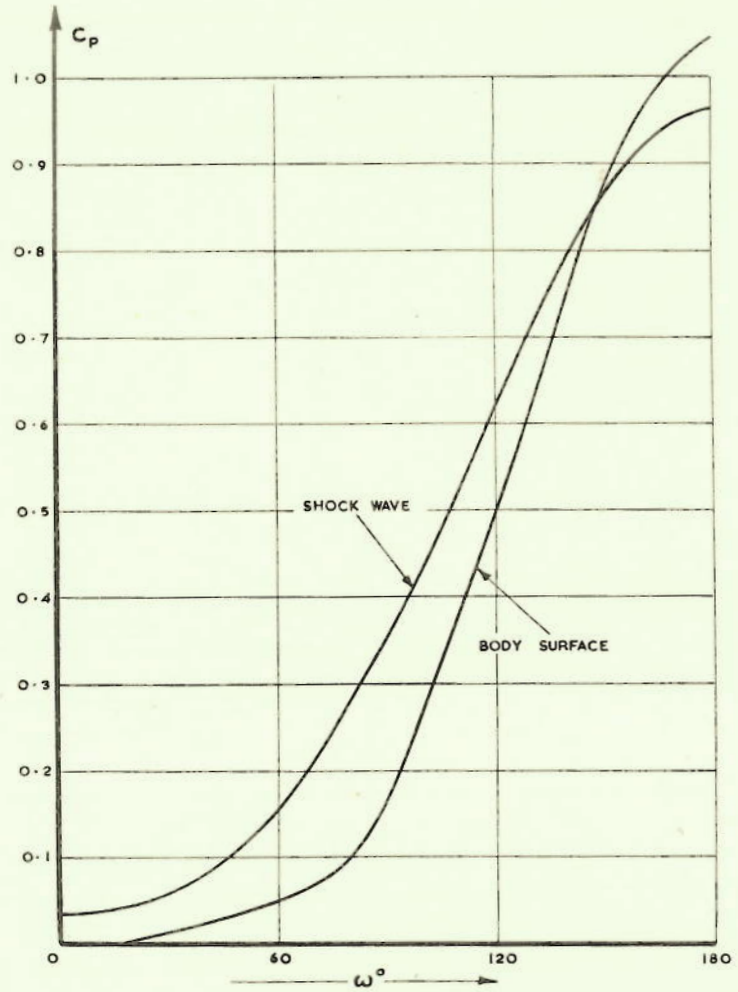

FIG. 14. FLOW BEHIND YAWED CONICAL SHOCK. PRESSURE DISTRIBUTION
M = 10 $\Psi_w = 30^\circ$ $\alpha = 20^\circ$ $C_P \sim \omega$

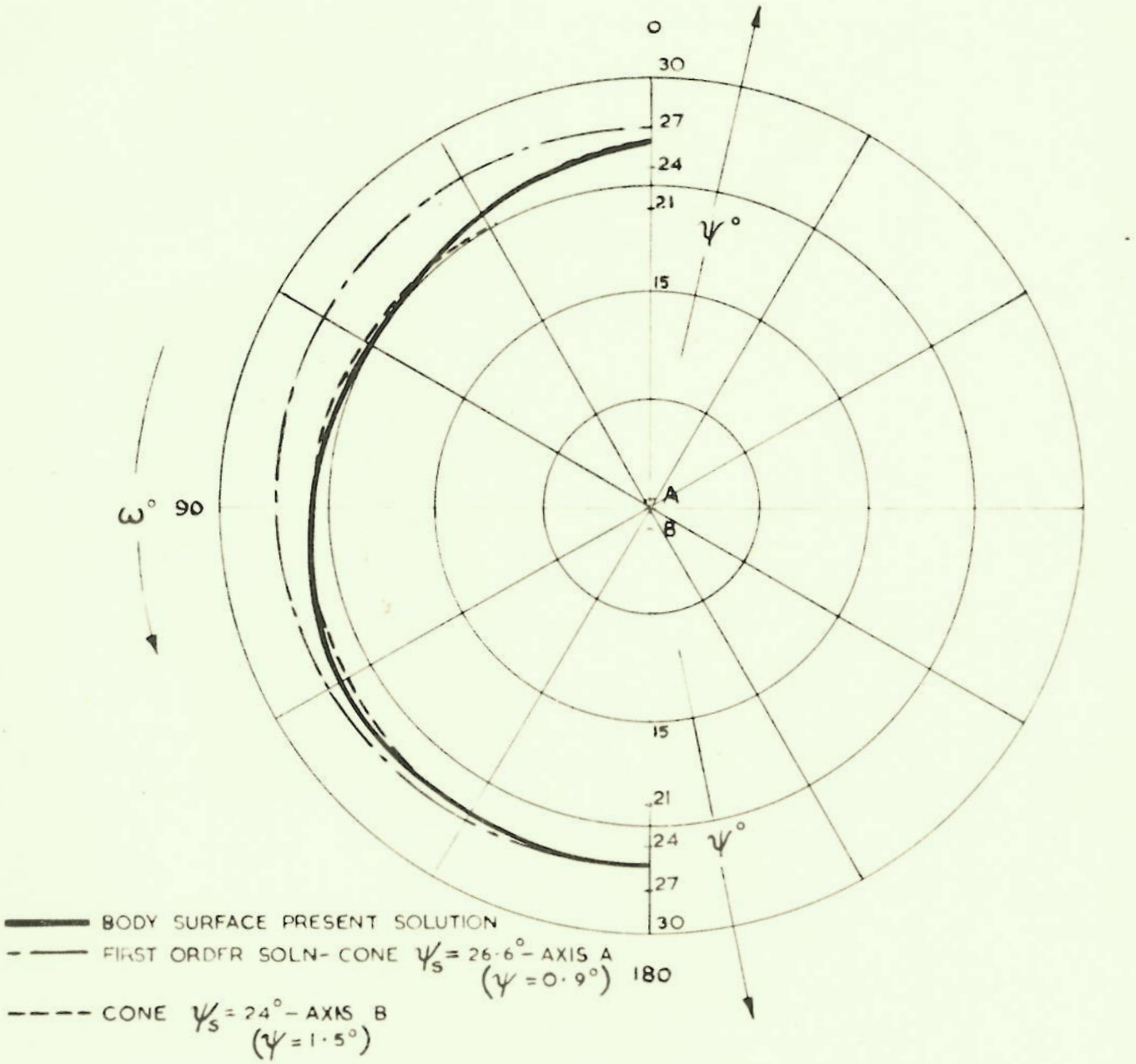

FIG. 15. FLOW BEHIND YAWED CONICAL SHOCK

$M_1 = 10$ $\psi = 30^\circ$ $\alpha = 20^\circ$ COMPARISON OF BODY WITH 1ST ORDER SOLN.